Available online at www.sciencedirect.com

ScienceDirect

Journal of Fluorine Chemistry 128 (2007) 317–331

JOURNAL OF FLUORINE CHEMISTRY

www.elsevier.com/locate/fluor

Review

Structural characteristics of alkylimidazolium-based salts containing fluoroanions

Kazuhiko Matsumoto [a,*], Rika Hagiwara [b]

[a] Department of Chemistry, McMaster University, 1280 Main Street, Hamilton, Ontario L8S 4M1, Canada
[b] Graduate School of Energy Science, Kyoto University, Yoshida, Sakyo-ku, Kyoto 606-8501, Japan

Received 1 September 2006; received in revised form 24 October 2006; accepted 26 October 2006
Available online 2 November 2006

Abstract

An overview of recent structural studies on alkylimidazolium-based salts containing fluoroanions is presented. Alkylimidazolium cations have been most extensively used for syntheses of ionic liquids (room temperature molten salts) because they usually exhibit low melting points, low viscosities and high conductivities. This review mainly focuses on structures of alkylimidazolium-based salts combined with a fluorocomplex anion ($(FH)_nF^-$, BF_4^-, PF_6^-, AsF_6^-, SbF_6^-, NbF_6^-, TaF_6^-), $N(SO_2CF_3)_2^-$ ($TFSI^-$) and $OSO_2CF_3^-$. The first part describes crystal structures of these salts and the second part describes computational, spectroscopic and diffraction studies on their liquid structures. Related studies on ionic liquids of non-alkylimidazolium cation and non-fluoroanion are also briefly summarized.

Keywords: Ionic liquid; Structure; Room temperature molten salt; Fluoroanion; Alkylimidazolium

---

Contents

---

1. Introduction

More than 10 years have passed since the term of ionic liquid was widely accepted. The initial report in this field, the discovery of ethylammonium nitrate (mp 285 K) by Walden in 1914, did not attract much attention [1]. In the 1970s and 80s, halogenoaluminate ionic liquids were studied mainly for electrochemistry [2–5]. In the 1990s, a number of moisture-stable ionic liquids, most containing fluorine, were synthesized and characterized [2,6–15]. Since ionic liquids are nonvolatile at ambient conditions, nonflammable and ionically conductive in wide temperature range, the use of ionic liquids immediately spread into various fields in electrochemistry [6,7,16], synthetic and catalytic chemistry [2,8–15]. Today, the term

---

* Corresponding author at: Department of Chemistry, McMaster University, 1280 Main Street, Hamilton, Ontario L8S 4M1, Canada.
Tel.: +1 905 525 9140x22537; fax: +1 905 525 2509.
E-mail address: matsumk@mcmaster.ca (K. Matsumoto).

0022-1139/$ – see front matter © 2006 Elsevier B.V. All rights reserved.
doi:10.1016/j.jfluchem.2006.10.016

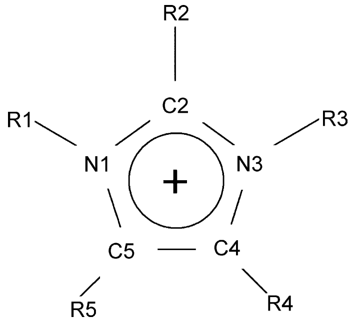

Fig. 1. Structure of alkylimidazolium cation.

"ionic liquid" is analogous to the terms "room temperature molten salt" or "ambient temperature molten salt" usually containing an organic cation. However, previously "ionic liquid" meant "liquid made of only ions regardless of temperatures" [17,18].

Among the organic cations known to form ionic liquids, alkylimidazolium cations have been studied the most in detail. This is because alkylimidazolium-based salts usually exhibit low melting points and low viscosities that normally lead to high conductivities. These excellent properties of alkylimidazolium-based salts are often explained by charge delocalization on the aromatic five-membered ring (Fig. 1).

Various ionic liquids containing fluoroanions are comprehensively reviewed in a recent paper by Xue et al. [8]. The higher stability of fluoroanion-based ionic liquids in air enables their use in various fields. The partial structures of ionic liquids, often discussed in terms of "ion pair" or "aggregate" of molecular level, give plausible explanations for physical properties, electrochemical processes and various reactions that take place in ionic liquids. The invention of the ionic liquid containing a fluoroanion, $EMImBF_4$ (EMIm = 1-ethyl-3-methylimidazolium), was made in 1992 [19] and therefore their structural characteristics have been rapidly reported for the recent 10 years. This review is focused on structural characteristics of alkylimidazolium-based salts especially containing fluoroanions.

2. Crystal structures of alkylimidazolium-based salts containing fluoroanions

One of the common approaches to study the structure of an ionic liquid is to start from its solid-state structure. Table 1 gives selected crystallographic data and melting points of fluoroanion-containing alkylimidazolium salts. Abbreviations for the names of the ion used in the present review are also summarized in the footnote of Table 1.

2.1. Fluorocomplex salts

As is found in some literature, alkylimidazolium salts of naked fluoride ion, F^-, have been reported to be unstable at ambient conditions [20–22]. The monohydrate salt, $BMImF{\cdot}H_2O$ (BMIm = 1-butyl-3-methylimidazolium), was obtained as a crystalline decomposition product from the hydrolytic degradation of $BMImPF_6$ [23]. In $BMImF{\cdot}H_2O$, $BMIm^+$ cations associate as dimers via overlapping alkyl tails, making up parallel sides of a box. Hydrogen bonds are observed between the hydrogen atoms of the cation or H_2O and F^-.

For the salt $DMImPF_6$ (DMIm = 1,3-dimethylimidazolium), the DMIm cations form a weakly hydrogen bonded zigzag chain motif via methyl hydrogen atoms and π-electron [24]. Hexafluorophosphate anions are located between these chains with closest contacts to the methyl hydrogen atoms. The structure of $DMImPF_6{\cdot}0.5C_6H_6$ (benzene) isolated on cooling the molten 1:2 $DMImPF_6$–benzene liquid contains a three-dimensional hydrogen bonding network in which isolated benzene molecules are contained [24]. The structure of $DMImPF_6$–benzene mixtures in the liquid state was studied by neutron diffraction based on this result [25].

Structures of a series of EMIm fluorocomplex salts have been successively reported after the initial structural report on $EMImPF_6$ [26]. Fig. 2 shows the layered structure of EMImFHF which contains the smallest fluorocomplex anion FHF^- in the series [27], and was studied as a structural model of a series of highly conductive ionic liquids, $RMIm(FH)_{2.3}F$ (RMIm: 1-alkyl-3-methylimidazolium) [28–32]. The flat imidazolium rings are stacked and arranged in parallel with the interlayer distance of 3.376 Å which is close to the van der Waals layer separation found in the graphite structure (3.35 Å). In each layer, very short hydrogen bond distances between the H atom of the cation ring and the F atoms of the anion (1.951, 2.166 and 2.226 Å) are observed. They are comparable to those observed in $BMImF{\cdot}H_2O$ (1.96, 2.07, 2.31 and 2.44 Å) [23]. A similar layered structure with an interlayer distance of 3.381 Å was reported for $EMImNO_2$ that contains slightly bigger and bent ONO^- anion [19]. In the $EMImBF_4$ structure, EMIm cations form a pillar with the β-carbon of the ethyl group sticking out of the imidazolium-ring plane [33,34]. The H(methylene)···π interaction sustains the cation–cation

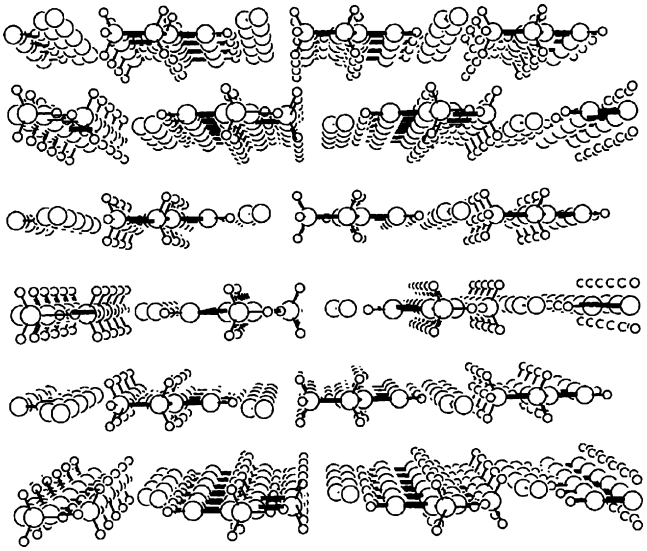

Fig. 2. Layered structure of EMImFHF viewed perpendicular to the *b*-axis [27], reproduced by permission of Elsevier.

Table 1
Structural parameters and melting points of alkylimidazolium salts containing fluoroanions

Salt[a]	Cell parameters[b]					T_m (K)[b]	References
	S.G.	V (Å^3)	Z	D_c (g cm^{-3})	T (K)		
$\mathrm{DMIm^+PF_6^-}$	$Pbca$	1894	8	1.698	173	–	[24]
$\mathrm{DMIm^+PF_6^-{\cdot}0.5C_6H_6}$	$P2_1/c$	1176.2	4	1.588	150	–	[24]
$\mathrm{DMIm^+TFSI^-}$	P-1	1417.0	4	1.769	173	295	[55]
$\mathrm{EMIm^+FHF^-}$	$P2_1/m$	395.09	2	1.262	298	324	[27]
$\mathrm{EMIm^+BF_4^-}$	$P2_1/c$	906.8	4	1.450	100	288	[33]
	$P2_1/n$	929.68	4	1.41	173	271.7	[34]
$\mathrm{EMIm^+PF_6^-}$	$P2_1/c$	1092.02	4	1.558	283–303	333	[26]
$\mathrm{EMIm^+AsF_6^-}$	$P2_1/c$	1123.04	4	1.775	298	326	[21]
$\mathrm{EMIm^+SbF_6^-}$	$P2_1/c$	1138.8	4	2.024	200	283	[21]
$\mathrm{EMIm^+NbF_6^-}$	$P2_12_12_1$	1124	4	1.880	200	272	[33]
$\mathrm{EMIm^+TaF_6^-}$	$P2_12_12_1$	1124.9	4	2.398	200	275	[33]
$\mathrm{EMIm^+Li^+_2\ (TFSI^-)_3}$	$P2_1/c$	3561.2	4	1.801	298	–	[59]
$\mathrm{EMImTFSI{\cdot}C_6H_6}$	$P2_1/n$	1989.6	4	1.567	110	288	[57]
$\mathrm{BMIm^+F^-{\cdot}H_2O}$	$P2_12_12_1$	995.7	4	1.176	173	–	[23]
$\mathrm{BMIm^+PF_6^-}$	P-1	610.2	2	1.55	180	274.9	[34]
	P-1	604.96	2	1.560	173	284	[36]
$\mathrm{BMIm^+OSO_2CF_3^-}$	$P2_1/n$	2883.2	8	1.33	200	279.7	[34]
$\mathrm{BMIm^+BARF^-}$	$P2_1/n$	8625.3	8	1.544	200	375–377	[61]
$\mathrm{PNMIm^+PF_6^-}$	P-1	597.1	2	1.642	140	348	[41]
$\mathrm{PNDMIm^+PF_6^-}$	P-1	650.7	2	1.578	140	358	[41]
$\mathrm{BDMIm^+BF_4^-}$	$P2_1/c$	2491.79	8	1.307	213	312.8	[37]
$\mathrm{BDMIm^+PF_6^-}$	Cc	1310.4	4	1.512	213	313.0	[37]
$\mathrm{BDMIm^+SbF_6^-}$	$P2_1/n$	1457.27	4	1.773	293	317.5	[37]
$\mathrm{TEIm^+TFSI^-}$	$P2_1/n$	1803	4	1.597	173	330	[55]
$\mathrm{DBIm^+OSO_2CF_3^-}$	$Pbca$	3240.9	8	1.354	150	–	[60]
$\mathrm{Me_3NBH_2MIm^+TFSI^-}$	P-1	922.0	2	1.564	173	333.2	[54]
$\mathrm{EtOC(O)CEtIm^+TFSI^-}$	$P2_1/c$	1871.91	4	1.644	223	318	[58]
$\mathrm{EMBzIm^+TFSI^-}$	$P2_1/n$	2061	4	1.552	295	323	[53]
$\mathrm{(DMImMCp)_2Fe^{2+}(PF_6^-)_2}$	P-1	641.6	1	1.797	84	Dec.[c]	[42]
$\mathrm{DisoPDMIm^+BF_4^-}$	$P4_32_12$	1416.9	4	1.257	293	410	[186]
$\mathrm{(MBz)_2Im^+BF_4^-}$	$P2_12_12_1$	1801.85	4	1.343	150	383	[39]
$\mathrm{(MBz)_2Im^+PF_6^-}$	$P2_12_12_1$	1916.40	4	1.464	100	381	[39]
$\mathrm{C_{12}MIm^+PF_6^-}$	$P2_1/a$	2000.7	4	1.32	123	333	[43]
$\mathrm{C_{14}MIm^+PF_6^-}$	$P2_1/a$	2204.84	4	1.279	175	348[d]	[44]

[a] DMIm: 1,3-dimethylimidazolium, EMIm: 1-ethyl-3-methylimidazolium, BMIm: 1-butyl-3-methylimidazolium, PNMIm: 1-methyl-3-propylnitrileimidazolium, PNDMIm: 1,2-dimethyl-3-propylnitrileimidazolium, BDMIm: 1-butyl-2,3-dimethylimidazolium, TEMIm: 1,2,3-triethylimidazolium, DBIm: 1,3-di-*tert*-butylimidazolium, $\mathrm{Me_3NBH_2MIm}$: (*N*-methylimidazole)(trimethylamine)boronium, EtOC(O)CEtIm: 1-(1-(*R*)-ethoxycarbonyl-ethyl)-3-methyl-imidazolium, EMBzIm: 1-ethyl-2-methy-3-benzyl-imidazolium, $\mathrm{(DMImMCp)_2Fe}$: 1,1′-bis{[1-(2,3-dimethyl)imidazolium]methyl}ferrocene, DisoPDMIm: 1,3-di-*iso*-propyl-4,5-dimethyl-imidazolium, $\mathrm{(MBz)_2Im}$: 1,3-di-*R*-(+)-methylbenzyl-imidazolium, $\mathrm{C_{12}MIm}$: 1-dodecyl-3-methylimidazolium, $\mathrm{C_{14}MIm}$: 1-methyl-3-tetradecylimidazolium, TFSI: bis(trifluoromethylsulfonyl)amide and BARF: tetrakis(3,5-bis(trifluoromethyl)phenyl)borate.

[b] S.G.: space group, V: cell volume, Z: number of formula units in the unit cell, D_c: density calculated from cell parameters, T: data collection temperature and T_m: melting point.

[c] Dec.: decomposition without melting.

[d] Crystalline to smectic phase transition.

interactions with a contact distance of 2.86 Å between the H atom in methylene group and the imidazolium ring centroid. A similar H(methylene)···π contact (2.86 Å) was also found in the $\mathrm{(EMIm)_2PtCl_6}$ structure [35]. Tetrafluoroborate anions also form a pillar along the *b*-axis. For EMIm salts of hexafluorocomplex anions, $\mathrm{EMImAsF_6}$ and $\mathrm{EMImSbF_6}$ are isostructural with $\mathrm{EMImPF_6}$ [21,26], whereas $\mathrm{EMImNbF_6}$ and $\mathrm{EMImTaF_6}$ exhibit a different structure [33]. Fig. 3 shows the ion packings in $\mathrm{EMImAsF_6}$ and $\mathrm{EMImNbF_6}$. In the $\mathrm{EMImAsF_6}$ structure, $\mathrm{EMIm^+}$ and $\mathrm{AsF_6^-}$ stack alternately along the *b*-axis to form pillars. On the other hand, in the $\mathrm{EMImNbF_6}$ structure, the anion appears in a zigzag arrangement along the *a*-axis where the nearest fluorine atoms have a distance of 3.441 Å (for F5···F2) and the cations adopt a pillar-like stacking along the same axis. Hydrogen bonds often play an important role in melting points of organic compounds. For the EMIm salts of fluorocomplex anions above, in spite of closer H···F contacts in $\mathrm{EMImNbF_6}$ and $\mathrm{EMImTaF_6}$ than those in $\mathrm{EMImPF_6}$, $\mathrm{EMImAsF_6}$ and $\mathrm{EMImSbF_6}$, the melting points of the former two compounds are much lower than those of the latter three compounds. $\mathrm{EMImBF_4}$ also exhibits a low melting point despite relatively strong hydrogen bonds in its lattice. These observations suggest that the strength of hydrogen bonding is not always a decisive factor in their melting points.

Currently, only one crystal structure of a BMIm fluorocomplex salt is known [34,36]. The compound $\mathrm{BMImPF_6}$, whose structure has been most extensively studied by various methods, contains two types of interplanar arrangements of

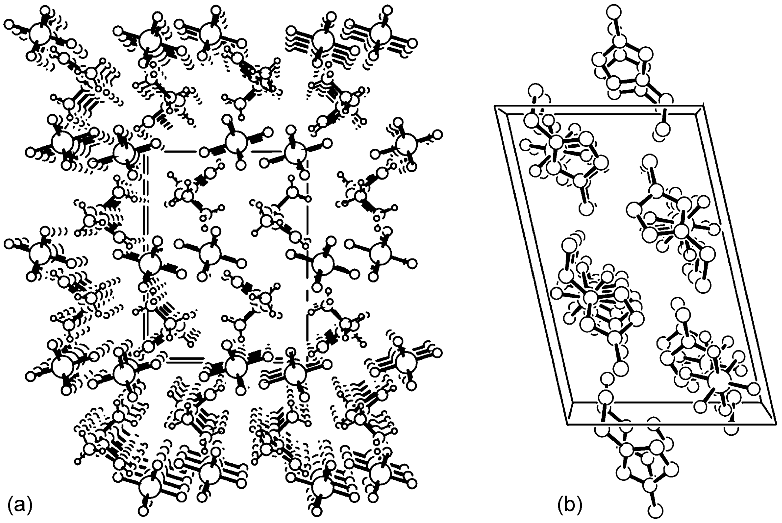

Fig. 3. Molecular packing in the structures of: (a) $EMImNbF_6$ and (b) $EMImAsF_6$ [33], reproduced by permission of Elsevier.

imidazolium cations. In one set, the butyl groups point into the space between the imidazolium rings, and in the other they point outwards. These pairs propagate continuously in the $BMImPF_6$ structure. There are no close π–π interactions between the imidazolium rings. The PF_6 anions are positioned close to the imidazolium rings and lie in the channels between the imidazolium rings and butyl chains. Existence of some hydrogen bonding was confirmed between H atoms of the cation and F atom of the anion in the lattice.

Crystal structures of a series of BDMIm (BDMIm = 1-butyl-2,3-dimethylimidazolium) salts combined with BF_4^-, PF_6^- and SbF_6^- were determined as structural models for ionic liquids [37]. In $BDMIm^+$, a methyl group is substituted for the most acidic C2 hydrogen atom. All three salts have significantly different structures and $BDMIm^+$ adopts different conformations in the different compounds with respect to the butyl chain that sticks out of the plane of the imidazolium ring. In $BDMImBF_4$, both the two crystallographically independent BF_4 anions are disordered at 213 K. This structure is composed of two different types of double layers. The anionic parts of these two layers are very similar, whereas the cationic part is markedly different. None of the hydrogen atoms within the imidazolium ring shows an orientation, which would suggest hydrogen bonding to the F atom of BF_4^-. The crystal structure of $BDMImPF_6$ is composed of alternating layers of cations and anions along the crystallographic (0 1 1) plane. All imidazolium ring planes are coplanar and all butyl chains aligned in one direction; both roughly parallel to the *a*-axis. The PF_6^- is ordered at 213 K but disordered at 298 K. In its ordered state, it is surrounded by six cations with the centers forming a distorted trigonal prism. No disorder is observed for the $BDMImSbF_6$ structure even at ambient temperature. The cation and anion arrangement in $BDMImSbF_6$ is reminiscent of NiAs-type structure, with the SbF_6 anions surrounded by six nearest neighbor cations in a distorted trigonal prismatic coordination and the cations surrounded by six SbF_6 anions in a distorted octahedral arrangement. There are no short contacts between carbon atoms of the butyl chains, and thus short-range repulsive interactions between the cations are further diminished with respect to the PF_6 salt. The structures of BDMIm salts of other non-fluoroanions, as well as their hydrogen bonding properties, has been discussed previously [38].

Solid-state structural models for ionic liquids containing fluorocomplex anions have also been reported for $(MBz)_2Im$ ($(MBz)_2Im$ = 1,3-di-*R*-(+)-methylbenzyl-imidazolium) salts [39]. Crystallographic structures of the two salts $(MBz)_2ImBF_4$ and $(MBz)_2ImPF_6$ are similar, where the cation is surrounded by six anions in both the salts. These structures resemble the $BMImBPh_4$ (BPh_4 = tetraphenylborate) structure [40]. As shown in Fig. 4, the cations form a network structure in the lattice, and the anions align as chains along the *a*-axis for $(MBz)_2ImBF_4$ and along the *b*-axis for $(MBz)_2ImPF_6$. The BF_4 salts has slightly longer C–H···F bonds with respect to the PF_6^-, while in the PF_6 salt the C–H donors are directed more linearly toward the F atoms. There are hydrogen bonds between the methyl group of the benzylic moiety and the F atoms in both salts. It was suggested that the general structural organization of the dialkylimidazolium salts in the solid state can be represented as $\{[(DAI)_3(X)]^{2+}[(DAI)(X)_3]^{2-}\}_n$, where DAI is the dialkylimidazolium cation and X is the anion.

A series of alkylimidazolium salts with a nitrile functional group added to the alkyl side-chain were reported, where crystal structures of two PF_6 salts, $PNMImPF_6$ (PNMIm = 1-methyl-3-propylnitrileimidazolium) and $PNDMImPF_6$ (PNDMIm = 1,2-dimethyl-3-propylnitrileimidazolium) were determined [41]. The compound $PNMImPF_6$ contains a short H···F contact of 2.43 Å at C2 and some other weaker hydrogen bonds. The $PNDMImPF_6$ salt also contains a short H···F contact of 2.49 Å at C5 although $PNDMImPF_6$ does not have the acidic C2 hydrogen atom.

Among a series of ferrocene-containing ionic liquids, the crystal structure of $(DMImMCp)_2Fe^{2+}(PF_6^-)_2$ ($(DMImMCp)_2Fe^{2+}$ = 1,1′-bis{[1-(2,3-dimethyl)imidazolium]methyl}ferrocene) was determined as a structural model of them [42]. In $(DMImMCp)_2Fe^{2+}(PF_6^-)_2$, the Cp–Fe–Cp angle is 180° and

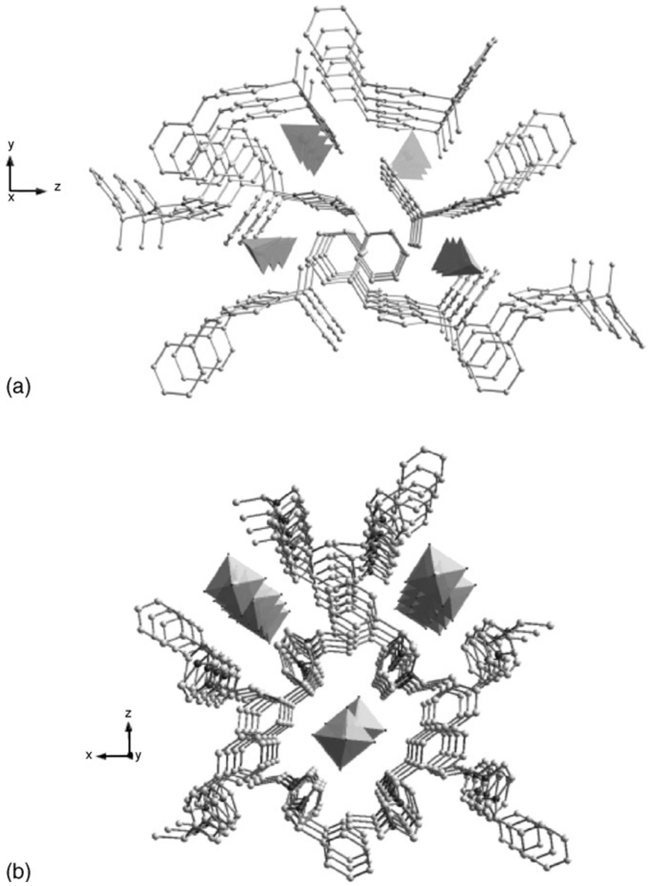

Fig. 4. View of the crystal structure of: (a) $(MBz)_2ImBF_4$ along the *b*-axis and (b) $(MBz)_2ImPF_6$ along the *c*-axis [39], reproduced by permission of American Chemical Society. Hydrogen atoms are omitted for clarity; BF_4^- and PF_6^- are shown as tetrahedra and octahedra, respectively.

the substituents on the Cp ring have a *trans*-arrangement. The PF_6^- is separated from the ferrocenyl cation in the lattice.

One of the interesting applications of ionic liquids is their use as liquid crystalline materials [43–47]. Crystal structures of dialkylimidazolium salts with long alkyl side-chains provide structural models for ionic liquid crystals. The crystal structure of $C_{12}MImPF_6$ ($C_{12}MIm$ = 1-dodecyl-3-methylimidazolium), which was reported in the study on a series of alkylimidazolium and alkylpyridinium-based ionic liquid crystalline materials, consists of discrete cations and anions separated by at least van der Waals distances [43]. The straight chain of the alkyl group is disrupted close to the ring where it adopts a bent conformation and exhibits a ‘‘spoon-shaped’’ structure. The chain configuration and the lack of any disorder in the structure appear to be consequences of the interdigitated molecular packing. As is often found for liquid crystalline salts, sheets of imidazolium rings and PF_6 anions are separated by alkyl chains parallel to each other (Fig. 5) with a spacing of 22.197(4) Å between the layers. According to X-ray powder diffraction studies for $RMImPF_6$ (R = C_{12}, C_{14}, C_{16} and C_{18}, where the subscript number represents the number of carbon atoms in the alkyl chain), a layered structure dominates them and the interlayer distance increases regularly with increasing length of the alkyl chain. Subsequent studies have revealed that $C_{14}MImPF_6$ has a similar structure to $C_{12}MImPF_6$ and a phase transition occurs at 278 K [44]. The phase transition does not involve a major structural change but is largely marked by an increase in the degree of motion in the anion and the alkyl chain on the cation. Studies on ionic liquid crystals were summarized in a recent review [47].

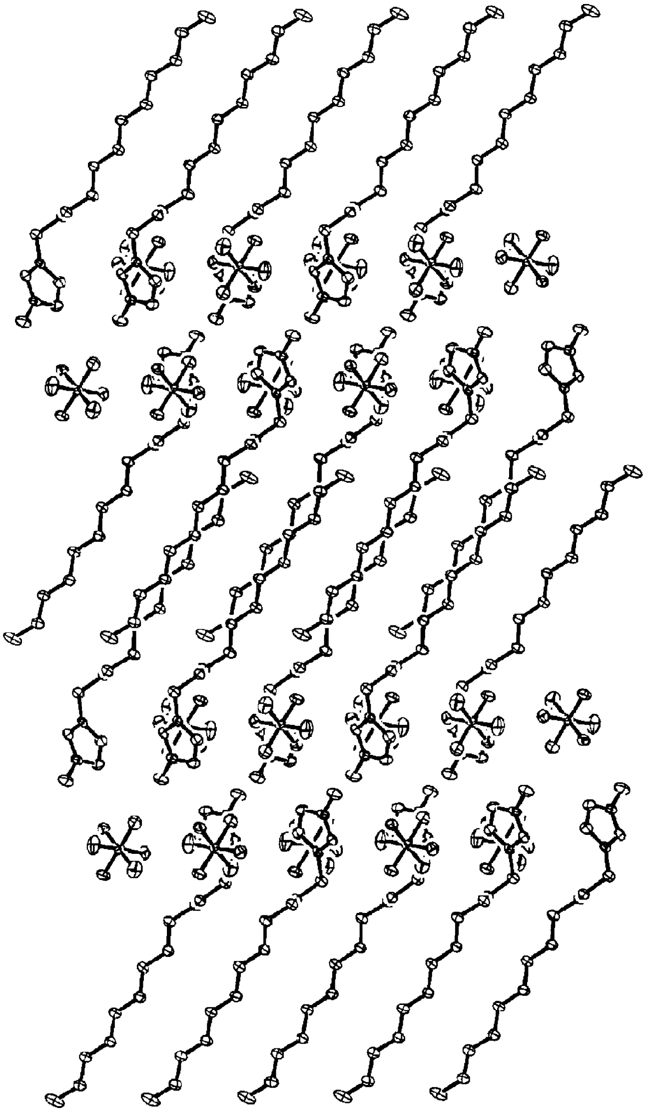

Fig. 5. Overall structure of $C_{12}MImPF_6$ showing the interdigitation and the tilted alkyl chains [43], reproduced by permission of The Royal Society of Chemistry.

2.2. $N(SO_2CF_3)_2^-$, $OSO_2CF_3^-$ and $BARF^-$ salts

Anions containing trifluoromethyl groups, $N(SO_2CF_3)_2^-$, $OSO_2CF_3^-$ and $BARF^-$ (BARF = tetrakis(3,5-bis(trifluoromethyl)phenyl)borate), have been used to synthesize ionic liquids and this section summarizes the crystal structures of alkylimidazolium salts containing these anions. The bis(trifluoromethylsulfonyl)amide anion ($N(SO_2CF_3)_2^-$ or $TFSI^-$) has been used as a counter ion of lithium salt, LiTFSI [48], an electrolyte of lithium (ion) batteries. It is one of the most popular anions for syntheses of ionic liquids that gives hydrophobic salts with low melting points, low viscosities and high electrical conductivities. The hydrophobicity is one of the important properties for non-distillable ionic liquids, which makes purifying and drying easier by solvent extraction. A series of alkylimidazolium salts combined with $TFSI^-$ were first reported in 1996 [49], followed by various $TFSI^-$-based ionic liquids [50–52].

The compound, EMBzImTFSI (EMBzIm = 1-ethyl-2-methyl-3-benzyl-imidazolium), is the first TFSI salt, which is related to ionic liquids whose structure has been determined by single-crystal X-ray diffraction [53]. In the EMBzImTFSI structure, $TFSI^-$ takes a *trans*-conformation and no strong hydrogen bonds between the cation and anion are observed. The S–N bond lengths of the anion in EMBzImTFSI (1.56–1.57 Å) are significantly shorter than typical S–N single bonds (~1.75 Å) as a result of the S–N–S charge delocalization. The key feature of this anion in promoting a low melting point in its compounds, concomitant with high fluidity, seems to be this charge delocalization coupled with the lack of hydrogen bonding. As in the case of EMBzImTFSI, the $Me_3NBH_2MImTFSI$ (Me_3NBH_2MIm = (*N*-methylimidazole)(trimethylamine)boronium) contains disordered TFSI anions in the *trans*-conformation and only weak intermolecular contacts in the lattice [54]. This is the first structural model of (*N*-alkylimidazole)(amine)boronium-based ionic liquids.

In DMImTFSI, both the two crystallographically distinct TFSI anions adopt a *cis*-conformation [55]. The crystal lattice of DMImTFSI consists of alternating two-dimensional sheets with an –AA–B–AA– pattern. These sheets are comprised of charge-bearing double layers of cations and anions separated by fluorous regions formed by the CF_3 groups on the anions. In the charged planes, the $TFSI^-$ is hydrogen-bonded to three equatorially arrayed 1,3-dimethylimidazolium cations through C–H···O and C–H···N contacts (Fig. 6) and to an additional imidazolium cation below each anion. Another structural model for TFSI-based salts is TEImTFSI (TEIm = 1,2,3-triethylimidazolium). The TEImTFSI structure consists of alternating layers of $TEIm^+$ cations and *trans*-TFSI anions with only weak cation–anion interactions [55]. The *cis*-conformation of $TFSI^-$ has a higher energy than the *trans*-conformation and therefore observed only in compounds where strong interaction between the cation and anion forces this conformation [55,56]. In DMImTFSI, hydrogen bond between ring hydrogen atoms of the cation and O atoms of the anion stabilizes the *cis*-conformation of the anion. The compound TEImTFSI contains fewer hydrogen bonds than DMImTFSI and the cation adopts a *trans*-conformation.

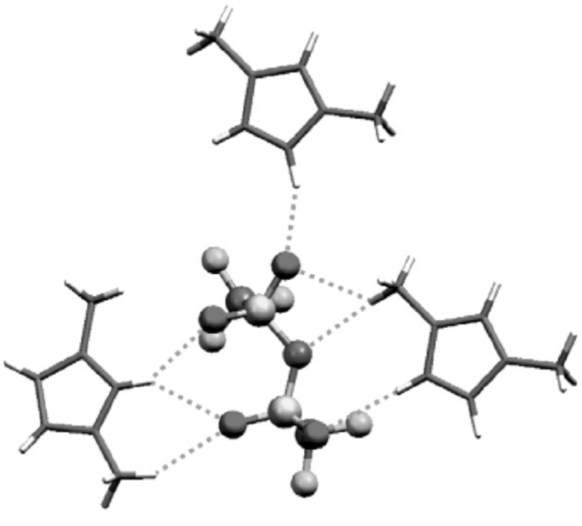

Fig. 6. Cation···anion hydrogen bonding in DMImTFSI, showing the three in-plane cations surrounding each anion resulting in the *cis*-anion conformation with all the CF_3 groups in each hydrogen-bonded sheet projecting from the same side of the layer [55], reproduced by permission of The Royal Society of Chemistry.

An equimolar inclusion compound obtained from the mixture of EMImTFSI and benzene, $EMImTFSI{\cdot}C_6H_6$, was characterized by single-crystal X-ray diffraction [57]. The interactions between the anion and the benzene molecule occur mainly between the hydrogen atoms of benzene and the oxygen atoms of the sulfonyl groups of the $TFSI^-$. Interactions with the fluorine atoms of the anion are also present at a lesser extent. As in the case of $DMImPF_6$, the anions cluster around the benzene molecule mainly in the plane of the aromatic ring and the interactions between the anion and benzene occur in that plane. The interactions between the imidazolium cations and benzene are mainly π–π interactions between aromatic rings. The interactions between the acidic hydrogen atoms in the cation and the π-electrons of benzene also exist, i.e. the cations occupy positions above and below the plane of the benzene aromatic ring. Some parts of this crystal structure resemble the structure of DMImTFSI shown above. However, the ionic network is more expanded in the case of the inclusion compound (it has to accommodate benzene molecules). Nevertheless, it manages to preserve a significant amount of its ion pair interactions.

The TFSI salt, EtOC(O)CEtImTFSI (EtOC(O)CEtIm = 1-(1-(*R*)-ethoxycarbonyl-ethyl)-3-methyl-imidazolium), is the first structural model of chiral ionic liquids [58]. Interestingly, a complete racemisation was observed for this compound. The $TFSI^-$ adopts a *cis*-conformation and two β-carbon atoms of the cation stick out of the imidazolium plane. Cations are surrounded by three TFSI anions and interact to the anions through some strong hydrogen bonds between hydrogen atoms of the cation and O or N atoms of the anion.

The crystal structure of $Li_2(EMIm)(TFSI)_3$ was determined as a structural model for ionic liquid electrolytes for lithium (ion) batteries [59]. Two of the three TFSI anions have *cis*-conformations and the third anion shows a *trans*-conformation. Both the crystallographically independent Li cations are trigonal-bipyramidally coordinated by five oxygen atoms of the anions, and no coordination by other atoms, such as nitrogen, is observed. The complicated Li···O local interactions form a two-dimensional network and $EMIm^+$ occupies a space in the network structure, weakly interacting with the anion. As a result of Li^+–$TFSI^-$ interactions, fluorine atoms on the CF_3 group form a so-called fluorous region.

Two examples of the crystal structures of alkylimidazolium salts containing the triflate anion ($OSO_2CF_3^-$) were reported. In the layered structure of $BMImOSO_2CF_3$ [34], the imidazolium ring of the cation and the SO_3-group of the anion are connected by hydrogen bonds to form a two-dimensional NaCl-like arrangement in each layer. The butyl group of the cation and the CF_3 group of the anion protrude out of the layer to the same direction. The butyl and CF_3 groups of the adjacent layer stick out to the opposite direction. Therefore, this structure contains a hydrophobic layer of the butyl and CF_3 group sandwiched between the two layers. The structure of $DBImOSO_2CF_3$ (1,3-di-*tert*-butylimidazolium) obtained by the reaction of $[Zn(t\text{-}BuNCHCHN\text{-}t\text{-}Bu)_2](OSO_2CF_3)_2$ and methanol was also reported [60].

The BMImBARF is a dialkylimidazolium salt containing tetraarylborate anion [61]. There is a typical disorder in the trifluoromethyl groups in the $BARF^-$. The *n*-butyl chain of the imidazolium cation is also disordered. There appears to be no hydrogen bond interactions between the H atom of cation and the π-electron of $BARF^-$. Unlike $BMImBPh_4$, the bulky trifluoromethyl moieties prevent the anion and cation from coming into close enough proximity for such interactions to occur [40].

2.3. Related studies

Structural studies of alkylimidazolium salts containing non-fluoroanions are briefly summarized here. Crystal structures of some halide salts, often used as starting materials to synthesize ionic liquids, have been determined [38,62–71]. Structures of alkylimidazolium chlorocomplex and oxychlorocomplex salts in the solid state are known; $AlCl_4^-$ [72] $CoCl_4^{2-}$, $NiCl_4^{2-}$ [73], $PtCl_4^{2-}$, $PtCl_6^{2-}$, $IrCl_6^{2-}$ [35], $PdCl_4^{2-}$ [74], $PdCl_4^{2-}\cdot H_2O$ [75], $[SnCl_3^-][Cl^-]$ [76], $AuCl_4^-$ [77], $LaCl_6^{3-}$ [78], $[FeCl_4^{2-}][FeCl_4^-]_2$ [38], $Cu_3Cl_8^-$ [79], $BiCl_4^-$ [80], $VOCl_4^{2-}$ [81], UCl_6^{2-} and $UO_2Cl_4^{2-}$ [82]. Structural data of the alkylimidazolium salts of the following anions, $AlBr_4^-$ [65], $Ru_2Br_9^{3-}$ [83], $Ag(CN)_2^-$ [84], NO_3^-, NO_2^- [19], $CH_3SO_4^-$ [85], HSO_3^- [38] $RB_{11}X_mH_n^-$ (R: alkyl, X: Br or I) [86], $SO_4^{2-}\cdot H_2O$ [19], $S_2O_7^-$ [87], BPh_4^- [39,40], $UO_2(NO_3)_4^{2-}$, $[\{UO_2(NO_3)_2\}_2(\mu\text{-}C_2O_4)]^{2-}$, $[\{UO_2(NO_3)_2\}_2(\mu\text{-}C_2O_4)]^{2-}\cdot NO_3^-$ and $[\{UO_2(NO_3)_2\}_2(\mu\text{-}C_2O_4)]^{2-}$·(ethanenitrile) [88] are also available.

Nonaromatic heterocyclic cations, such as alkylpyrrolidinium and alkylpiperidinium as well as linear tetraalkylammonium, have attracted attention due to the needs of more chemically and electrochemically stable compounds [16,89–91]. Compared to the cases of aromatic cations, nonaromatic cation-based salts generally exhibit higher melting points. However, room temperature ionic liquids are obtained when they are combined with some suitable anions such as $TFSI^-$. Some nonaromatic cation-based salts of PF_6^- [92], $TFSI^-$ [93,94], $N(SO_2CH_3)_2^-$ [95] and SCN^- [96] related to ionic liquids are characterized by single crystal X-ray diffraction.

3. Computational, spectroscopic and diffraction studies on liquid structures of alkylimidazolium-based salts containing fluoroanions

In order to gain insight into liquid structures of ionic liquids, the solid-state structures of related compounds are studied. A number of computational, spectroscopic and diffraction studies have also been conducted on ionic liquids by many groups. Since an ionic liquid usually contains a large organic cation, which is not in a simple spherical shape, local ion–ion interactions in the liquid state are not straightforward. Table 2 summarizes the computational, spectroscopic and diffraction studies on ion–ion interactions and liquid structures of alkylimidazolium-based ionic liquids containing fluoroanions. Abbreviations for the names of ions, which do not appear in Table 1 are given in the footnote of Table 2.

3.1. Computational approaches

Molecular dynamics (MD) and Monte-Carlo simulations are popular methods to study the structures of ionic liquids. Although these studies usually include important computational details necessary for the simulations such as a force field [97–99], only the results of ion–ion interactions obtained from the simulations are summarized in this section. The results of MD simulations on $EMImBF_4$ and $BMImBF_4$ as well as $EMImAlCl_4$ and $BMImAlCl_4$ suggest that the local structural features are strongly affected by the nature of the anion [100,101]. The cation–anion radial distribution functions (RDF) show a more defined first solvation sphere of anions around the cations and vice versa in the $BMIm^+$-based ionic liquids than that in $EMIm^+$-based ionic liquids.

$BMImPF_6$ is the most experimentally studied and simulated ionic liquid to date. Monte-Carlo simulation for $BMImPF_6$ using a united atom force field combined with *ab initio* calculation suggests that the cation–anion pairs tend to order in a first solvation shell at a separation of about 4 Å [102]. Subsequent cation–anion solvation shells occur at 10 and 17 Å. Long range order persists even beyond 20 Å, as evidenced by the fact that the RDF still shows oscillations. Such a long range order is not observed for non-polar liquids, but is expected here, due to the strong Coulombic interactions in the system. The anion tends to associate with the C2 hydrogen atom of the cation. A similar distribution of anion was observed in the MD simulation of $DMImPF_6$ [103]. Radial distribution function obtained by MD simulations of $BMImPF_6$ shows the presence of a long spatial correlation of more than 20 Å [104]. The cation–anion correlation has a sharp peak around 4.2 Å (C2–P distance) and appears to be stronger than cation–cation and anion-anion correlations. Another report on the same system using MD simulations gives similar RDFs [105,106]. In addition, comparison of the results of simulations using two united atom force fields and one all atom force-field shows that the RDFs based on each force-field differ from each other (Fig. 7) [107]. All the three force fields show a strong localization of the anion about the C2 carbon, whereas the localization states of the anion about the other two ring hydrogen atoms, C4 and C5, depend on the choice of the force-field. Another simulation for $BMImPF_6$ which gives similar RDFs to those above suggest that a ring π–π stacking exists and the conformation of the butyl chain has three minima in the potential energy function at the N1–C7–C8–C9 dihedral angle

Table 2
Computational, spectroscopic and diffraction studies on ion–ion interactions and liquid structures of alkylimidazolium-based room temperature ionic liquids containing fluoroanions

Method	Salt[a]	References[b]
Calculation	$DMIm^+BF_4^-$	(MO·DFT) [111]
	$DMIm^+PF_6^-$	(MD) [103,110,151]; (MO·DFT) [103,110,111,151]
	$EMIm^+(HF)_{2.3}F^-$	(MD) [115]; (MO·DFT) [127]
	$EMIm^+BF_4^-$	(MD) [101,110,142]; (MO·DFT) [101,110,111, 114,136,137]
	$EMIm^+PF_6^-$	(MD) [142]; (MO·DFT) [111,114,138]
	$EMIm^+OCOCF_3^-$	(MO·DFT) [114]
	$EMIm^+OSO_2CF_3^-$	(MD) [142]; (MO·DFT) [114]
	$EMIm^+TFSI^-$	(MD) [142]; (MO·DFT) [114]
	$EDMIm^+BF_4^-$	(MO·DFT) [114]
	$MPIm^+BF_4^-$	(MO·DFT) [111,137]
	$MPIm^+PF_6^-$	(MD) [142]; (MO·DFT) [111,138]
	$BMIm^+BF_4^-$	(MD) [110,142]; (MO·DFT) [111,137]
	$BMIm^+PF_6^-$	(MD) [104–106,108–110, 142,151]; (MC) [102,107] (MO·DFT) [101,102,104–108, 110–113,138,139,151]
	$BMIm^+OCOCF_3^-$	(MO·DFT) [109]
	$BMIm^+OCOC3F_7^-$	(MO·DFT) [109]
	$BMIm^+OSO_2CF_3^-$	(MO·DFT) [109]
	$BMIm^+OSO2C4F_9^-$	(MO·DFT) [109]
	$BMIm^+TFSI^-$	(MD) [142]
	$HMIm^+PF_6^-$	(MD) [142]; (MO·DFT) [139]
	$C_{12}MIm^+PF_6^-$	(MD) [142]
NMR	$DMIm^+(HF)_{2.3}F^-$	[127]
	$DMIm^+TFSI^-$	[124]
	$EMIm^+(HF)_{2.3}F^-$	[127]
	$EMIm^+BF_4^-$	[118,119,122,130]
	$EMIm^+PF_6^-$	[130]
	$EMIm^+TFSI^-$	[122,124]
	$MPIm^+(HF)_{2.3}F^-$	[127]
	$BMIm^+(HF)_{2.3}F^-$	[127]
	$BMIm^+BF_4^-$	[120,123,128–131]
	$BMIm^+PF_6^-$	[120,121,123,126,128–130]
	$BMIm^+OCOCF_3^-$	[123]
	$BMIm^+OSO2CF_3^-$	[123]
	$BMIm^+TFSI^-$	[123,124,128]
	$BMIm^+N(SO_2C_2F_5)_2^-$	[123]
	$MPeIm^+(HF)_{2.3}F^-$	[127]
	$HMIm^+(HF)_{2.3}F^-$	[127]
	$HMIm^+TFSI^-$	[124]
	$MOIm^+BF_4^-$	[130]
	$MOIm^+PF_4^-$	[130]
	$MOIm^+TFSI^-$	[124]
	$(MBz)_2Im^+BF_4^-$	[39]
	$(MBz)_2Im^+PF_6^-$	[39]
IR Raman	$EMIm^+BF_4^-$	[136,137,140]
	$EMIm^+PF_6^-$	[138,140]
	$EMIm^+OSO_2CF_3^-$	[140]
	$EMIm^+TFSI^-$	[140,141]
	$MPIm^+BF4^-$	[137]
	$MPIm^+PF6^-$	[138]
	$BMIm^+BF4^-$	[66,135,137]
	$BMIm^+PF6^-$	[138,139]
	$HMIm^+PF6^-$	[139]
X-ray diffraction	$EMIm^+FHF^-$	[146]
	$MIm^+(HF)_{2.3}F^-$	[147]
	$EMIm^+(HF)_{2.3}F^-$	[146,147]
	$BMIm^+(HF)_{2.3}F^-$	[147]
	$HMIm^+(HF)_{2.3}F^-$	[147]
Neutron diffraction	$DMIm^+PF_6^-$	[149]
	$DMIm^+TFSI^-$	[150]

[a] MIm: 1-methylimidazolium, MPIm: 1-methyl-3-propylimidazolium, MPeIm: 1-methyl-3-pentylimidazolium, HMIm: 1-hexyl-3-methylimidazolium and MOIm: 1-methyl-3-octylimidazolium.

[b] MD: molecular dynamics simulation, (MC): Monte-Carlo simulation and (MO·DFT) *ab initio* molecular orbital and DFT calculations.

of 180, −60, and +60, corresponding to one trans and two equivalent gauche conformers [108].

Ionic conductivities of a series of BMIm-based ionic liquids combined with fluorinated organic anions (CF_3COO^-, $C_3F_7COO^-$, $OSO_2CF_3^-$, and $C_4F_9SO_3^-$) as well as PF_6^- were investigated by MD simulations [109]. The result shows that the self-diffusion coefficient is an important factor in determining the conductivity of ionic liquid. The RDF for $BMImPF_6$ shows that two solvation shells are located at 4.4 and 10.8 Å. On the other hand, for the other ionic liquids containing fluorinated organic anions, the first solvation shell was located at a greater distance and the second solvation shell was located at 10–12 Å.

Geometries of the isolated ions and ion pairs for ionic liquids composed of alkylimidazolium cations ($DMIm^+$, $EMIm^+$ and $BMIm^+$) and fluorocomplex anions (BF_4^- and PF_6^-) were calculated by molecular mechanics and *ab initio* methods [110]. The geometry of $DMIm^+$–PF_6^- ion pair has an

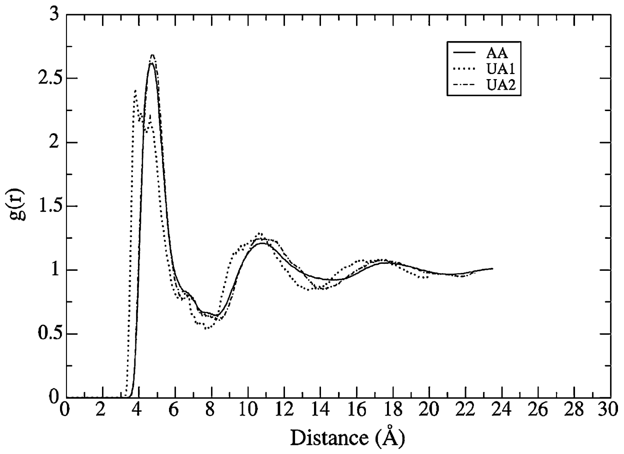

Fig. 7. Center of mass radial distribution functions for the cation and anion obtained from the three force fields at 298 K [107], reproduced by permission of Elsevier. AA: all atom force-field [105], UA1: united atom force-field 1 [102] and UA2 united atom force-field 2 [107].

asymmetric structure with the H···F interaction via both H atoms of the imidazolium ring and the alkyl side-chain. Similar geometries are also obtained for $EMIm^+–BF_4^-$ and $BMIm^+PF_6^-$ ion pairs. This kind of model was also observed in other *ab initio* or DFT calculations [111–113]. Molecular mechanics based on the proposed force-field gives similar results to those from the *ab initio* calculations by the adjustment of some parameters. Molecular dynamics simulation for $BMImPF_6$ using the same force field results in a little difference in the cation–anion RDF from those described above, giving the two solvation cell located at 4.8 and 11.0 Å which are longer than those in the other reports above. The RDFs for F atom of PF_6^- and H atoms of $BMIm^+$ indicate that the order of hydrogen bonding activities of the different H atoms on the C atoms in the cation is $H2 > H4, H5 > H6 > HC$, where H6 denotes H atoms in the butyl chain bound to N atom and HC denotes the other H atoms in the butyl chain. Comparison of the results for various anions reveals that the interaction between the C2 hydrogen atom and X ($X = Cl^-$ or F atom in BF_4^- and PF_6^-) decreases in the order $Cl^- > BF_4^- > PF_6^-$. According to the visualized pictures of the special distribution functions (SDFs), which show intuitively the three-dimensional probability distribution of the atoms of interest around a central ion, there are mainly three regions of the anion distributed around the cation in the first solvation shell.

Ab initio calculation of a series of EMIm-based salts reveals that the magnitude of the interaction energies of the ion pair follows the trend $OCOCF_3^- > BF_4^- > OSO_2CF_3^- > (CF_3SO_2)_2N^- > PF_6^-$ [114]. Most of the stable models for the ion pairs containing $EMIm^+$ have an interaction via the C2 hydrogen atom, whereas BF_4^- in the $EDMIm^+–BF_4^-$ (EDMIm = 1-ethyl-2,3-dimethyimidazolium) ion pair is located at a position closer to the center of the imidazolium ring. The small difference in the interaction energies between $EMIm^+$ and $EDMIm^+$ shows that hydrogen bonding via the C2 hydrogen atom of the imidazolium ring is not essential for the attraction between the ring and anion. Comparing the experimental ion conductivities shows that the magnitude and directionality of the interaction energy between ions play a crucial role in determining the ionic dissociation/association dynamics in these ionic liquids (see Section 3.2).

The structure of $EMIm(FH)_{2.3}F$ was simulated by MD [115]. As shown above and below, this system has been studied by single-crystal X-ray diffraction in the solid state (for EMImFHF, see Section 2.1 and Fig. 2), pulsed-gradient spin-echo NMR (see Section 3.2) and high energy X-ray diffraction (see Section 3.4). The MD simulation confirmed that short-range stacking of the cations does exist but there is no evidence of layer formation. The experimental X-ray diffraction spectra are quite well reproduced by this model. A similar imidazole-HF system was also investigated by *ab initio* molecular orbital and density functional theory methods [116].

Some other computational studies combined with experimental vibrational spectroscopy are summarized in Section 3.3.

3.2. NMR spectroscopy

NMR spectroscopy is an effective method for studying the ion–ion interactions in liquids, including ionic liquids. In some earlier work on alkylimidazolium chloroaluminate salts, the ring hydrogen atoms, especially the one at the C2 position, shift upfield in the ^1H NMR spectra, as Cl^- is replaced by $AlCl_4^-$. This means that the hydrogen atoms are more shielded by stronger hydrogen bonds to the anion and the chemical shift moves accordingly [4,117]. On the other hand, two magnetically shielded cones above and below the imidazolium ring influences the chemical shift of the hydrogen atoms that penetrate into these cones and shifts it to the upfield [117]. The effects of these two phenomena were compared in ^1H NMR spectra of acetone solutions of some EMIm salts at different concentrations [49]. For the salts containing more basic anions such as acetate, the chemical shift of the most acidic C2 hydrogen atom sharply increases with an increase in concentration. This is because an increase of salt concentration results in stronger hydrogen bonds to the anion and the effect of the negatively charged atom in the anion on the chemical shift is stronger than that of the neighboring imidazolium ring. In the cases with less basic anions such as $TFSI^-$, the chemical shift decreases when the concentration increases, because the hydrogen bonds to the anion are weaker and the effect of the neighboring imidazolium ring is enhanced.

The diffusion coefficients of $EMIm^+$ measured by pulsed field gradient NMR for $EMImBF_4$ indicates that a structural change occurs at around 335 K, which is supported by ^{11}B quadrupolar relaxation rates [118,119]. This structural change was ascribed to the transformation of the diffusion particle from ‘discrete ion-pair’ to ‘individual ion’. The mean radii for diffusing spheres in the two phases, calculated using the Stokes–Einstein equation, are 2.79 Å in the region of ion pair and 1.90 Å in the region of individual ion. A similar observation was reported for $BMImBF_4$ and $BMImPF_6$ [120]. Analysis of ^{13}C dipole–dipole relaxation rates by NMR spectroscopy identified the formation of hydrogen bond (C2–H···F) between $BMIm^+$ and BF_4^-. According to the NMR measurements combined with results of some physical property and IR spectroscopy measurements, the $BMImBF_4$ exists in an ion-pair (quasi-molecular) state below 279 K and $BMImPF_6$ does between 273 and 353 K. The authors also state that those ionic liquids form ‘extended hydrogen bonding network’ at higher temperature regions. In another report [121], the reorientational dynamics of $BMImPF_6$ were studied by the measurement of ^{13}C spin-lattice relaxation rates and nuclear overhauser effect (NOE) factors by NMR. Discontinuities in the relaxation curves were not observed for the neat $BMImPF_6$ sample. The presence of a hydrogen bond between the C2 hydrogen atom and F atom was confirmed by the dynamic method.

The cation–anion association in a number of ionic liquids was also studied by using the pulsed-field gradient spin-echo NMR (PGSE-NMR) technique [122–125]. The molar conductivities of ionic liquids calculated from the diffusion coefficients obtained by the PGSE-NMR technique via the

Nernst–Einstein equation, Λ_{NMR}, are larger than those obtained by AC impedance measurements, Λ_{imp}. This phenomenon is explained by ion-pairing between the cation and anion, which reduces the charge carrier concentration in the liquid and hence, the ionic conductivity. For a series of BMIm-based ionic liquids, the $\Lambda_{\mathrm{imp}}/\Lambda_{\mathrm{NMR}}$ ratio follows the order $\mathrm{BMImPF_6} > \mathrm{BMImBF_4} > \mathrm{BMIm(C_2F_5SO_2)_2N} > \mathrm{BMImTFSI} > \mathrm{BMImOSO_2CF_3} > \mathrm{BMImOCOCF_3}$ at 30 °C. Since the cationic structure is the same for this series of salts, the change in ratio depends merely on the anionic species. In addition, a study of a series of 1-alky-3-methyllimidazolium TFSI salts shows that the $\Lambda_{\mathrm{imp}}/\Lambda_{\mathrm{NMR}}$ ratio decreases with an increasing number of carbon atoms in the alkyl chain. For $\mathrm{BMImPF_6}$, the hydrodynamic volumes, V_{D} ($=N_{\mathrm{A}}4\pi r^3/3$), observed for both the cation and anion by PGSE-NMR were much smaller than the van der Waals' molar volumes, V_{vdW} [126], which indicates the smaller friction. There is a lot of free space in $\mathrm{BMImPF_6}$, as evident in a comparison of calculated molar volumes. The molar volume ($V_{\mathrm{m}} = M/\rho$) calculated by dividing the molar mass by the density is 0.205 $\mathrm{cm^3\,mol^{-1}}$ at 293 K, which is much larger than the total van der Waals' molar volume (0.122 $\mathrm{cm^3\,mol^{-1}}$) of the cationic and anionic species. The free space could make a negative contribution to the effective friction and this negative effect is observed more remarkably for the cation than for the anion in view of $V_{\mathrm{D}}/V_{\mathrm{vdW}}$.

For a highly conductive ionic liquid, $\mathrm{RMIm(FH)_{2.3}F}$ [28–32], the existence of cation–anion associations was also suggested by PGSE-NMR. The aggregates of ordered ions, $\mathrm{A(AX)}_m{}^{+}$ and $\mathrm{(AX)}_n\mathrm{X}^{-}$ (A = cation and X = anion) can frequently change their form and size by inserting and extracting some mono-ions at the surface [127]. A similar model was proposed for $\mathrm{(MBz)_2ImBF_4}$, $\mathrm{PF_6}$ and $\mathrm{BPh_4}$ by ^{1}H NMR, combined with conductivity and microcalorimetric measurements [39]. Recent $\{^1\mathrm{H}\}^{19}\mathrm{F}$-HOESY (heteronuclear overhauser effect spectroscopy) studies on $\mathrm{BMImBF_4}$, BMImTFSI and $\mathrm{BMImPF_6}$ revealed that the anion does not occupy a specific position in these salt [128]. Moreover, in dichloromethane where the PGSE data show almost complete ion pairing, there are strong, non-selective NOE contacts between the cation and anion. This eliminates hydrogen bonding as the primary source of interaction between the cation and anion, as this would lead to selectivity in the HOESY contacts. A structural motif for $\mathrm{BMImBF_4}$, in which the $\mathrm{BF_4}^-$ straddles the imidazolium plane was proposed. On the other hand, in methanol solution, the solvent surrounds the ions and the cation–anion contacts are reduced.

The chemical shifts in ^{1}H NMR spectra of $\mathrm{BMImBF_4}$ and $\mathrm{BMImPF_6}$ were determined in various deuterated solvents [129]. The results show that the chemical shifts of the ring hydrogen atoms of $\mathrm{BMImPF_6}$ are more sensitive to solvation than those of $\mathrm{BMImBF_4}$. The interaction of ring hydrogen atoms with relatively small and basic $\mathrm{BF_4}^-$ is closer than the larger and less basic $\mathrm{PF_6}^-$. For both cases, the C2 hydrogen atom has a stronger interaction to the anion than the others. The chemical shifts in both ^{1}H and ^{13}C NMR spectra were also reported for a series of 1-alkyl-3-methylimidazolium salts containing $\mathrm{BF_4}^-$ and $\mathrm{PF_6}^-$ in various solvents [130]. Cation-cation, cation-water and cation–anion interactions in the $\mathrm{BMImBF_4\text{-}H_2O}$ mixture were studied by NMR spectroscopy through the NOE [131]. The homonuclear NOE experiments indicated that the structure of pure $\mathrm{BMImBF_4}$ changes upon hydration to a different form with a lower degree of ring stacking (or other types of piling). In other words, the presence of water makes the imidazolium–imidazolium associations weaker and the methyl group shifts progressively towards the most hydrophobic part of the imidazolium ion, namely the *n*-butyl chain, as the water content rises. At very low water concentrations, the water–cation hydrogen bonding interactions are very specific and localized at ring hydrogen atoms. At higher water content, the interaction of water with other hydrogen atoms in the side chains increases and no preference is shown. The heteronuclear NOE experiments indicate the existence of tight ion pairs in the pure liquid, even in the presence of small amounts of water, and in DMSO solution [132].

3.3. Vibrational spectroscopy

Vibrational spectroscopy has been employed to obtain information about inter-molecular interaction in ionic liquids. The C-H stretching bands of ring hydrogen atoms in the region between 3050 and 3100 $\mathrm{cm^{-1}}$ have conventionally been used as a criterion for strong hydrogen bonding [21,26,65,133–136].

Hydrogen bonded structures of $\mathrm{BMImPF_6}$ as well as $\mathrm{DMImCH_3SO_4}$ were studied by high pressure IR spectroscopy [135]. The results indicate that the peak frequencies of the alkyl and imidazolium C–H stretching bands have a non-monotonic pressure dependence. They blue-shift initially, then undergo no change, and blue-shift again upon increasing the pressure. This discontinuity in frequency shift is similar to the trend observed for a $\mathrm{DMImCH_3SO_4/D_2O}$ mixture. The $\mathrm{BMImPF_6}$ results indicate the existence of C–H···F interactions between the F atoms of the $\mathrm{PF_6}^-$ and the ring H atoms of the cation. Additional hydrogen bond-like interactions were also observed between $\mathrm{PF_6}^-$ and the H atoms on the alkyl side-chains.

Recent reports on intermolecular interactions in ionic liquids using vibrational spectroscopy are usually combined with computational techniques. The structure of the ion pair in $\mathrm{EMImBF_4}$ was described by *ab initio* and DFT calculations [136]. Only one final structure was obtained, independent of the method used. Unlike the chloride systems, where $\mathrm{Cl^-}$ is found in the plane of the imidazolium ring of the cation, the $\mathrm{BF_4}^-$ is positioned over the ring and has short contacts not only with the C2 hydrogen atom of the cation, but also with a hydrogen atom of the methyl group. The computations reveal that normal modes of the $\mathrm{EMIm^+}\text{–}\mathrm{BF_4}^-$ ion pair rather closely resemble those of the isolated ions. There are a few exceptions, notably the antisymmetric B–F stretching vibrations of the anion, and out-of-plane and stretching vibrations of the C2–H moiety of the cation. The drastic increase of the C2–H out-of-plane frequency of $\mathrm{EMIm^+}$ in the course of ion-pair formation is strongly indicative of hydrogen bonding. However, the experimental IR spectra of neat and $\mathrm{CD_2H_2}$ solution of

$EMImBF_4$ were almost identical. In all likelihood, the cation and anion are held together mainly by powerful Coulombic attractions and hydrogen bonding plays only a minor role. In another paper [137], DFT and RHF calculations reproduced Raman and IR spectra of $EMImBF_4$, $MPImBF_4$ and $BMImBF_4$, using appropriate correction factors. Theoretical (DFT) alkyl side-chain conformational changes in the three ionic liquids have only a limited effect on the theoretical gas phase vibrations. The ion pair models suggest hydrogen bonds not only between the F atoms of the anion and the C2 hydrogen atom on the imidazolium ring, but also between the F atoms of the anion and H atoms on the adjacent alkyl side chains in all polymorphic structures (Fig. 8). Investigations of the vibrational spectra of $EMImPF_6$, $MPImPF_6$ and $BMImPF_6$ were made in the same manner [138]. Raman spectra of $BMImPF_6$ and $HMImPF_6$ were also assigned using *ab initio* calculation in another report [139]. The results indicate that almost equal amounts of two conformers are observed. Two polymorphs of BMImCl, one which contains all anti conformers for the butyl chain, and the other which contains one gauche, exist in $BMImPF_6$, as proposed in a previous study [66]. Similar results were obtained for the analogous two conformers in $HMImPF_6$. The analysis of the HMImCl–$HMImPF_6$ binary system shows that neither the changes in hydrogen bonding to the ring hydrogen atoms nor the change in Coulombic environment have a detectable effect upon the essentially 50:50 distribution of the two conformers. This conformational equilibrium of $EMIm^+$ in $EMImBF_4$, $EMImPF_6$, $EMImOSO_2CF_3$ and EMImTFSI was also studied through a combination of Raman spectroscopy and theoretical calculations [140]. According to this report, the $EMIm^+$ exists as either a nonplanar (C2-N1-C6-C7 = 110°) or planar (C2–N1–C6–C7 = 0°) conformer in the ionic liquids and that the anionic environment hardly influences the equilibrium. On the other hand, the conformational equilibrium of $TFSI^-$ in EMImTFSI that was investigated in the same way suggests that two conformers with two C–S–N–S dihedral angles of (90.9°, 90.9°) and (−81.2°, 120.2°) exist in the ionic liquid [141]. In another paper, dihedral distribution functions obtained by MD simulation for alkyl side-chains of various 1-alkyl-3-methylimidazolium salts combined with BF_4^-, PF_6^- and $TFSI^-$ [142] also indicated the existence of some conformers for the alkyl side-chains in the liquid states.

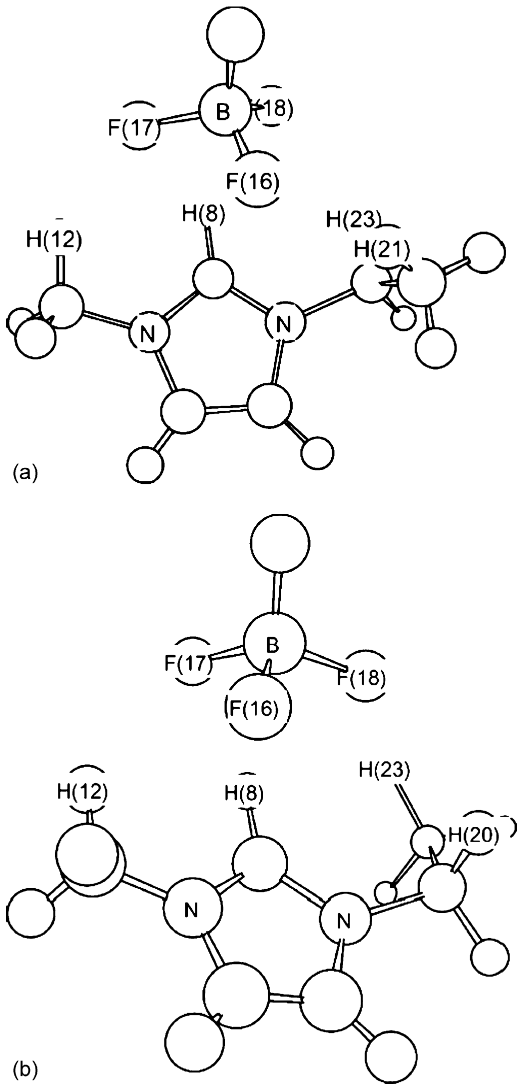

Fig. 8. (a) Molecular structure of $EMImBF_4$ (B3LYP/6-311 + G(2d,p))—conformer 1. Hydrogen bonds include: F17–H12 = 2.214 Å; F17–H8 = 2.199 Å; F16–H8 = 2.610 Å; F16–H21 = 2.353 Å; F18–H8 = 2.003 Å and F18– H23 = 2.381 Å. (b) Molecular structure of $EMImBF_4$ (B3LYP/6-311 + G(2d,p))—conformer 2. Hydrogen bonds include: F16–H8 = 2.697 Å; F17–H12 = 2.355 Å; F17–H8 = 1.952 Å; F18–H8 = 2.321 Å; F18–H20 = 2.580 Å and F18–H23 = 2.477 Å [137], reproduced by permission of Elsevier.

The molecular state of water in various alkylimidazolium-based ionic liquids was also investigated by means of IR spectroscopy [143,144] and near infra-red spectroscopy [145].

3.4. X-ray and neutron diffraction

Since X-ray and neutron diffraction provide a direct picture of the average structure of liquid, they are powerful techniques to elucidate the liquid structures of ionic liquids. However, X-ray and neutron diffraction data on the structures of ionic liquids are limited thus far most likely due to the experimental difficulties. Structures of EMImFHF and $RMIm(FH)_{2.3}Fs$ were studied by high energy X-ray diffraction [146,147]. The X-ray diffraction patterns of liquid EMImFHF and $EMIm(HF)_{2.3}F$ were similar to each other with a first sharp diffraction peak at $Q = 1.85\ \text{Å}^{-1}$. This peak does not correspond to the ones in the calculated intra-molecular form factors for isolated $EMIm^+$ and $(HF)_nF^-$ ($n = 2$ and 3). However, the peak position coincides with the (0 0 2) diffraction peak in the powder X-ray pattern of solid EMImFHF, which corresponds to the layered structure (see Section 2.1 and Fig. 2), which suggests that such a layered structure may be partially preserved in the liquid state. All other $RMIm(FH)_{2.3}F$ (R = hydrogen, butyl and hexyl) ionic liquids showed similar diffraction patterns, but the value of this first sharp diffraction peak shifts to lower diffraction angle with increasing alkyl side-chain length. This shift corresponds to a concomitant increase in inter-molecular distances in the ionic liquids.

The liquid structures of $DMImPF_6$ and DMImTFSI were analyzed by neutron diffraction and the results were compared to DMImCl [148–150]. The cation–cation contacts become larger as the size of the anion is increased: $Cl^- < PF_6^- < TFSI^-$. A similar trend is also seen for the cation–anion interactions. Although the anion shell is at a shorter distance from the central cation compared with the cation shells, the long-range alternating structure of cations and anions found in the DMImCl and $DMImPF_6$ does not exist in DMImTFSI. The probability distributions of the cation and anion around the cation shows the anion density axial to the ring decreases ($Cl^- > PF_6^- > TFSI^-$) whereas the opposite is true for the facial anion density ($Cl^- < PF_6^- < TFSI^-$). The $DMIm^+$ occupies the space where the anion does not exist: in other words, the cations and the anions occupy mutually exclusive positions. This is more pronounced in the liquid structure of DMImTFSI than in $DMImPF_6$. The crystal structure and the liquid structure of $DMImPF_6$ are very similar. For example, the large ''holes'' in the cation–cation distribution are found in both the liquid and solid states. Moreover, in both states, short cation–cation contacts are found between the methyl hydrogen atoms and the anion, which predominantly interacts with the ring and not the ring H atoms. On the other hand, comparison of the crystal structure and the liquid structure of DMImTFSI (see Section 2.2 and Fig. 6) indicates little correlation between the two. For example, the $TFSI^-$ adopts a *trans*-orientation predominantly in the liquid whereas a *cis*-orientation is found in the solid phase. The results for DMImCl and $DMImPF_6$ were corroborated by MD simulations [151].

3.5. Related studies

Many computational studies have been made on ionic liquids containing non-alkylimidazolium cations or non-fluoroanions and on mixtures of ionic liquids and solutes [22,152–175]. A number of experimental (NMR spectroscopy [176–179], vibrational spectroscopy [160,173,174,180–182] and neutron diffraction [148,161,183]) studies have also been employed for investigating structures of ionic liquids, except those mentioned above. Results of another interesting characterization method, electronspray ionization mass spectroscopy, have recently revealed that an ionic liquid can form aggregates and their size depends on the solvent used and the ionic liquid concentration [184,185].

4. Summary

This review summarizes structural studies of alkylimidazolium-based salts containing fluoroanions from the viewpoint of crystallographic, computational, spectroscopic and diffraction techniques. Crystallographic studies for various fluorocomplex salts show that hydrogen bonding is not always a decisive factor in melting points of ionic liquids. However, another factor such as lattice energy, related to the packing of ions, also influences melting points. In addition to cation–anion interactions, cation–cation interactions are often observed in some crystal structures. Structural determination of $TFSI^-$ salts reveals that $TFSI^-$ weakly interacts with the cations but there are still some strong interactions via O or N atoms. Most computational and diffraction approaches to liquid structures of alkylimidazolium-based salts focuses on the coordination environment around an ion with varying quality of agreement with crystallographic studies. *Ab initio* MO and DFT calculations give a stable state of each ion or ion pair and are used to obtain initial states of MD and Monte Carlo simulations. Molecular dynamics and Monte Carlo simulations are widely used to simulate the structures of ionic liquids on a large scale. Depending on a computational method or a force-field used, slightly different RDFs are obtained for the same ionic liquid. There is a limitation to describe structures of ionic liquids by MD and Monte Carlo simulations at this stage and further progress is strongly expected in this field to design more excellent ionic liquids. The results of vibrational spectroscopy combined with computations suggest the existence of local hydrogen bonding and some preferable conformations of alkylimidazolium cations. According to some NMR spectroscopic studies, ion–ion association occurs in ionic liquids. This association is probably related to local hydrogen bonding, which is also indicated by the other techniques. A possible association state is the neutral ion pair composed of one cation and one anion or the larger charged or neutral ion aggregate composed of more than three ions since ionic liquids do not contain any solvent.

References

[1] P. Walden, Bull. Acad. Imper. Sci. (St. Petersburg) (1914) 405–422.
[2] C.M. Gordon, Appl. Catal. A 222 (2001) 101–117.
[3] J.S. Wilkes, J.A. Levisky, R.A. Wilson, C.L. Hussey, Inorg. Chem. 21 (1982) 1263–1264.
[4] A.A. Fannin Jr., L.A. King, J.A. Levisky, J.S. Wilkes, J. Phys. Chem. 88 (1984) 2609–2614.
[5] A.A. Fannin Jr., D.A. Floreani, L.A. King, J.S. Landers, B.J. Piersma, D.J. Stech, R.L. Vaughn, J.S. Wilkes, J.L. Williams, J. Phys. Chem. 88 (1984) 2614–2621.
[6] R. Hagiwara, Y. Ito, J. Fluor. Chem. 105 (2000) 221–227.
[7] R. Hagiwara, Electrochemistry 70 (2002) 130–136.
[8] H. Xue, R. Verma, J.M. Shreeve, J. Fluor. Chem. 127 (2006) 159–176.
[9] T. Welton, Chem. Rev. 99 (1999) 2071–2084.
[10] K.R. Seddon, J. Chem. Technol. Biotechnol. 68 (1997) 351–356.
[11] P. Wasserscheid, W. Kein, Angew. Chem. Int. Ed. 39 (2000) 3772–3789.
[12] J. Dupont, R.F. de Souza, P.A.Z. Suarez, Chem. Rev. 102 (2002) 3667–3692.
[13] H. Olivier-Bourbigou, L. Magna, J. Mol. Catal. A 182–183 (2002) 419–437.
[14] J.D. Holbrey, K.R. Seddon, Clean Prod. Proc. 1 (1999) 223–236.
[15] R. Sheldon, Chem. Commun. (2001) 2399–2407.
[16] H. Ohno (Ed.), Electrochemical Aspects of Ionic Liquids, John Wiley and Sons, Inc., New Jersey, 2005.
[17] K. Ui, M. Ueda, R. Hagiwara, M. Mizuhata, Yoyuen Oyobi Koon Kagaku 47 (3) (2004) 114–123.
[18] D. Inman, D. Lovering (Eds.), Ionic Liquid, Plenum Press, New York, 1981.
[19] J.S. Wilkes, M.J. Zaworotko, J. Chem. Soc., Chem. Commun. (1992) 965–967.
[20] K. Matsumoto, R. Hagiwara, Y. Ito, J. Fluor. Chem. 115 (2002) 133–135.
[21] K. Matsumoto, R. Hagiwara, R. Yoshida, Y. Ito, Z. Mazej, P. Benkič, B. Žemva, O. Tamada, H. Yoshino, S. Matsubara, Dalton Trans. (2004) 144–149.
[22] E.A. Turner, C.C. Pye, R.D. Singer, J. Phys. Chem. A 107 (2003) 2277–2288.

[23] R.P. Swatloski, J.D. Holbrey, R.D. Rogers, Green Chem. 5 (2003) 361–363.
[24] J.D. Holbrey, W.M. Reichert, M. Nieuwenhuyzen, O. Sheppard, C. Hardacre, R.D. Rogers, Chem. Commun. (2003) 476–477.
[25] M. Deetlefs, C. Hardacre, M. Nieuwenhuyzen, O. Sheppard, A.K. Soper, J. Phys. Chem. B 109 (2005) 1593–1598.
[26] J. Fuller, R.T. Carlin, H.C. De Long, D. Haworth, J. Chem. Soc., Chem. Commun. (1994) 299–300.
[27] K. Matsumoto, T. Tsuda, R. Hagiwara, Y. Ito, O. Tamada, Solid State Sci. 4 (2002) 23–26.
[28] R. Hagiwara, T. Hirashige, T. Tsuda, Y. Ito, J. Fluor. Chem. 99 (1999) 1–3.
[29] R. Hagiwara, T. Hirashige, T. Tsuda, Y. Ito, J. Electrochem. Soc. 149 (2002) D1–D6.
[30] R. Hagiwara, K. Matsumoto, Y. Nakamori, T. Tsuda, Y. Ito, H. Matsumoto, K. Momota, J. Electrochem. Soc. 150 (2003) D195–D199.
[31] R. Hagiwara, Y. Nakamori, K. Matsumoto, Y. Ito, J. Phys. Chem. B 109 (2005) 5445–5449.
[32] K. Matsumoto, R. Hagiwara, Y. Ito, S. Kohara, K. Suzuya, Nucl. Instrum. Meth. B. 199 (2003) 29–33.
[33] K. Matsumoto, R. Hagiwara, Z. Mazej, P. Benkič, B. Žemva, Solid State Sci. 8 (2006) 1250–1257.
[34] A.R. Choudhury, N. Winterton, A. Steiner, A.I. Cooper, K.A. Johnson, J. Am. Chem. Soc. 127 (2005) 16792–16793.
[35] M. Hasan, I.V. Kozhevnikov, M.R.H. Siddiqui, C. Femoni, A. Steiner, N. Winterton, Inorg. Chem. 40 (2001) 795–800.
[36] S.M. Dibrov, J.K. Kochi, Acta Cryst. C62 (2006) o19–o21.
[37] P. Kölle, R. Dronskowski, Eur. J. Inorg. Chem. (2004) 2313–2320.
[38] P. Kölle, R. Dronskowski, Inorg. Chem. 43 (2004) 2803–2809.
[39] C.S. Consorti, P.A.Z. Suarez, R.F. de Souza, R.A. Burrow, D.H. Farrar, A.J. Lough, W. Loh, L.H.M. da Silva, J. Dupont, J. Phys. Chem. B 109 (2005) 4341–4349.
[40] J. Dupont, P.A.Z. Suarez, R.F. de Souza, R.A. Burrow, J.P. Kintzinger, Chem. Eur. J. 6 (2000) 2377–2381.
[41] D. Zhao, Z. Fei, R. Scopelliti, P.J. Dyson, Inorg. Chem. 43 (2004) 2197–2205.
[42] Y. Gao, B. Twamley, J.M. Shreeve, Inorg. Chem. 43 (2004) 3406–3412.
[43] C.M. Gordon, J.D. Holbrey, A.R. Kennedy, K.R. Seddon, J. Mater. Chem. 8 (1998) 2627–2636.
[44] J. De Roche, C.M. Gordon, C.T. Imrie, M.D. Ingram, A.R. Kennedy, F. Lo Celso, A. Triolo, Chem. Mater. 15 (2003) 3089–3097.
[45] S. Kunsági-Máté, B. Lemli, G. Nagy, L. Kollár, J. Phys. Chem. B 108 (2004) 9246–9250.
[46] C.J. Bowlas, D.W. Bruce, K.R. Seddon, Chem. Commun. (1996) 1625–1626.
[47] K. Binnemans, Chem. Rev 105 (2005) 4148–4204.
[48] J.L. Nowinski, P. Lightfoot, P.G. Bruce, J. Mater. Chem. 4 (1994) 1579–1580.
[49] P. Bonhôte, A.-P. Dias, M. Armand, N. Papageorgiou, K. Kalyanasundaram, M. Grätzel, Inorg. Chem. 35 (1996) 1168–1178.
[50] R.P. Singh, S. Manandhar, J.M. Shreeve, Tetrahedron Lett. 43 (2002) 9497–9499.
[51] C.M. Jin, J.M. Shreeve, Inorg. Chem. 43 (2004) 7532–7538.
[52] D.R. MacFarlane, P. Meakin, J. Sun, N. Amini, M. Forsyth, J. Phys. Chem. B 103 (1999) 4164–4170.
[53] J.J. Golding, D.R. MacFarlane, L. Spiccia, M. Forsyth, B.W. Skelton, A.H. White, Chem. Commun. (1998) 1593–1594.
[54] P.A. Fox, S.T. Griffin, W.M. Reichert, E.A. Salter, A.B. Smith, M.D. Tickell, B.F. Wicker, E.A. Cioffi, J.S. Davis Jr., R.D. Rogers, A. Wierzbicki, Chem. Commun. (2005) 3679–3681.
[55] J.D. Holbrey, W.M. Reichert, R.D. Rogers, Dalton Trans. (2004) 2267–2271.
[56] L. Xue, C.W. Padgett, D.D. Desmarteau, W.T. Pennington, Solid State Sci. 4 (2002) 1535–1545.
[57] J. Łachwa, I. Bento, M.T. Duarte, J.N.C. Lopes, L.P.N. Rebelo, Chem. Commun. (2006) 2445–2447.
[58] J.J. Jodry, K. Mikami, Tetrahedron Lett. 45 (2004) 4429–4431.
[59] K. Matsumoto, R. Hagiwara, O. Tamada, Solid State Sci. 8 (2006) 1103–1107.
[60] E. Rijnberg, B. Richter, K.-H. Thiele, J. Boersma, N. Veldman, A.L. Spek, G. van Koten, Inorg. Chem. 37 (1998) 56–63.
[61] J. Finden, G. Beck, A. Lantz, R. Walsh, M.J. Zaworotko, R.D. Singer, J. Chem. Crystallogr. 33 (2003) 287–295.
[62] A.J. Arduengo, H.V.R. Dias, R.L. Harlow, M. Kline, J. Am. Chem. Soc. 114 (1992) 5530–5534.
[63] C.J. Dymek Jr., D.A. Grossie, A.V. Fratini, W.W. Adams, J. Mol. Struct. 213 (1989) 25–34.
[64] A.K. Abdul-Sada, A.M. Greenway, P.B. Hitchcock, T.J. Mohammed, K.R. Seddon, J.A. Zora, J. Chem. Soc., Chem. Commun. (1986) 1753–1754.
[65] A. Elaiwi, P.B. Hitchcock, K.R. Seddon, N. Srinivasan, Y.-M. Tan, T. Welton, J.A. Zora, J. Chem. Soc., Dalton Trans. (1995) 3467–3472.
[66] R. Ozawa, S. Hayashi, S. Saha, A. Kobayashi, H. Hamaguchi, Chem. Lett. 32 (2003) 948–949.
[67] S. Hayashi, R. Ozawa, H. Hamaguchi, Chem. Lett. 32 (2003) 498–499.
[68] S. Saha, S. Hayashi, A. Kobayashi, H. Hamaguchi, Chem. Lett. 32 (2003) 740–741.
[69] J.D. Holbrey, W.M. Reichert, M. Nieuwenhuyzen, S. Johnson, K.R. Seddon, R.D. Rogers, Chem. Commun. (2003) 1636–1637.
[70] J.L. Anderson, R. Ding, A. Ellern, D.W. Armstrong, J. Am. Chem. Soc. 127 (2005) 593–604.
[71] Z. Fei, D. Zhao, T.J. Geldbach, R. Scopelliti, P.J. Dyson, Chem. Eur. J. 10 (2004) 4886–4893.
[72] J.A. Boon, R.T. Carlin, A.M. Elias, J.S. Wilkes, J. Chem. Cryst. 25 (1995) 57–62.
[73] P.B. Hitchcock, K.R. Seddon, T. Welton, J. Chem. Soc., Dalton Trans. (1993) 2639–2643.
[74] M.F. Ortwerth, M.J. Wyzlic, R.G. Baughman, Acta Cryst. C54 (1998) 1594–1596.
[75] N. Kuhn, M. Göhner, M. Steimann, C. Nachtigal, Z. Kristallogr. NCS 214 (1999) 565–566.
[76] N. Kuhn, R. Fawzi, H. Kotowski, M. Steimann, Z. Kristallogr. 213 (1998) 435–436.
[77] M. Hasan, I.V. Kozhevnikov, M.R.H. Siddiqui, A. Steiner, N. Winterton, Inorg. Chem. 38 (1999) 5637–5641.
[78] K. Matsumoto, T. Tsuda, T. Nohira, R. Hagiwara, Y. Ito, O. Tamada, Acta Cryst. C58 (2002) m186–m187.
[79] H.J. Sun, K. Harms, J. Sundermeyer, Z. Kristallogr. 220 (2005) 42–44.
[80] D.J. Williams, W.T. Pennington, D. VanDerveer, J.T. Anderton, K.M. White, J. Chem. Cryst. 33 (2003) 465–472.
[81] P.B. Hitchcock, R.J. Lewis, T. Welton, Polyhedron 12 (1993) 2039–2044.
[82] P.B. Hitchcock, T.J. Mohammed, K.R. Seddon, J.A. Zora, C.L. Hussey, E.H. Ward, Inorg. Chim. Acta 113 (1986) L25–L26.
[83] D. Appleby, P.B. Hitchcock, K.R. Seddon, J.E. Turp, J.A. Zora, C.L. Hussey, J.R. Sanders, T.A. Ryan, J. Chem. Soc., Dalton Trans. (1990) 1879–1887.
[84] Y. Yoshida, K. Muroi, A. Otsuka, G. Saito, M. Takahashi, T. Yoko, Inorg. Chem. 43 (2004) 1458–1462.
[85] J.D. Holbrey, W.M. Reichert, R.P. Swatloski, G.A. Broker, W.R. Pitner, K.R. Seddon, R.D. Rogers, Green Chem. 4 (2002) 407–413.
[86] A.S. Larsen, J.D. Holbrey, F.S. Tham, C.A. Reed, J. Am. Chem. Soc. 122 (2000) 7264–7272.
[87] N. Kuhn, H. Bohnen, G. Henkel, Z. Kristallogr. 211 (1996) 57.
[88] A.E. Bradley, C. Hardacre, M. Nieuwenhuyzen, W.R. Pitner, D. Sanders, K.R. Seddon, R.C. Thied, Inorg. Chem. 43 (2004) 2503–2514.
[89] K. Matsumoto, R. Hagiwara, Y. Ito, Electrochem. Solid State Lett. 7 (2004) E41–E44.
[90] H. Matsumoto, H. Kageyama, Y. Miyazaki, Chem. Commun. (2002) 1726–1727.
[91] H. Matsumoto, M. Yanagida, K. Tanimoto, M. Nomura, Y. Kitagawa, Y. Miyazaki, Chem. Lett. 29 (2000) 922–923.
[92] J. Golding, N. Hamid, D.R. MacFarlane, M. Forsyth, C. Forsyth, C. Collins, J. Huang, Chem. Mater. 13 (2001) 558–564.
[93] W.A. Henderson, M. Herstedt, V.G. Young Jr., S. Passerini, H.C. De Long, P.C. Trulove, Inorg. Chem. 45 (2006) 1412–1414.
[94] C.M. Forsyth, D.R. MacFarlane, J.J. Golding, J. Huang, J. Sun, M. Forsyth, Chem. Mater. 14 (2002) 2103–2108.

[95] J.M. Pringle, J. Golding, K. Baranyai, C.M. Forsyth, G.B. Deacon, J.L. Scott, D.R. MacFarlane, New J. Chem. 27 (2003) 1504–1510.
[96] J.M. Pringle, J. Golding, C.M. Forsyth, G.B. Deacon, M. Forsyth, D.R. MacFarlane, J. Mater. Chem. 12 (2002) 3475–3480.
[97] P.A. Hunt, Mol. Simul. 32 (2006) 1–10.
[98] J.N. Canongia Lopes, J. Deschamps, A.A.H. Pádua, J. Phys. Chem. B 108 (2004) 2038–2047.
[99] J.N. Canongia Lopes, A.A.H. Pádua, J. Phys. Chem. B 108 (2004) 16893–16898.
[100] J. de Andrade, E.S. Böes, H. Stassen, J. Phys. Chem. B 106 (2002) 3546–3548.
[101] J. de Andrade, E.S. Böes, H. Stassen, J. Phys. Chem. B 106 (2002) 13344–13351.
[102] J.K. Shah, J.F. Brennecke, E.J. Maginn, Green Chem. 4 (2002) 112–118.
[103] C.G. Hanke, S.L. Price, R.M. Lynden-Bell, Mol. Phys. 99 (2001) 801–809.
[104] C.J. Margulis, H.A. Stern, B.J. Berne, J. Phys. Chem. B 106 (2002) 12017–12021.
[105] T.I. Morrow, E.J. Maggin, J. Phys. Chem. B 106 (2002) 12807–12813.
[106] J.H. Antony, D. Mertens, T. Breitenstein, A. Dölle, P. Wasserscheid, W.R. Carper, Pure Appl. Chem. 76 (2004) 255–261.
[107] J.K. Shah, E.J. Maginn, Fluid Phase Equilibr. 222–223 (2004) 195–203.
[108] N.M. Micaelo, A.M. Baptista, C.M. Soares, J. Phys. Chem. B 110 (2006) 14444–14451.
[109] S.U. Lee, J. Jung, Y.K. Han, Chem. Phys. Lett. 406 (2005) 332–340.
[110] Z. Liu, S. Huang, W. Wang, J. Phys. Chem. B 108 (2004) 12978–12989.
[111] K. Dong, S. Zhang, D. Wang, X. Yao, J. Phys. Chem. A 110 (2006) 9775–9782.
[112] Z. Meng, A. Dölle, W.R. Carper, J. Mol. Struct. (THEOCHEM) 585 (2002) 119–128.
[113] Y.U. Paulechka, G.J. Kabo, A.V. Blokhin, O.A. Vydrov, J.W. Magee, M. Frenkel, J. Chem. Eng. Data 48 (2003) 457–462.
[114] S. Tsuzuki, H. Tokuda, K. Hayamizu, M. Watanabe, J. Phys. Chem. B 109 (2005) 16474–16481.
[115] M. Salanne, C. Simon, P. Turq, J. Phys. Chem. B 110 (2006) 3504–3510.
[116] L. Gong, W. Guo, J. Xiong, R. Li, X. Wu, W. Li, Chem. Phys. Lett. 425 (2006) 167–178.
[117] A.G. Avent, P.A. Chaloner, M.P. Day, K.R. Seddon, T. Welton, J. Chem. Soc., Dalton Trans. (1994) 3405–3413.
[118] J.F. Huang, P.Y. Chen, I.W. Sun, S.P. Wang, Inorg. Chim. Acta 320 (2001) 7–11.
[119] J.F. Huang, P.Y. Chen, I.W. Sun, S.P. Wang, Spectrosc. Lett. 34 (2001) 591–603.
[120] P.A.Z. Suarez, S. Einloft, J.E.L. Dullius, R.F. Souza, J. Dupont, J. Chim. Phys. 95 (1998) 1626–1639.
[121] J.H. Antony, D. Mertens, A. Dölle, P. Wasserscheid, W.R. Carper, Chem. Phys. Chem. 4 (2003) 588–594.
[122] A. Noda, K. Hayamizu, M. Watanabe, J. Phys. Chem. B 105 (2001) 4603–4610.
[123] H. Tokuda, K. Hayamizu, K. Ishii, M.A.B.H. Susan, M. Watanabe, J. Phys. Chem. B 108 (2004) 16593–16600.
[124] H. Tokuda, K. Hayamizu, K. Ishii, M.A.B.H. Susan, M. Watanabe, J. Phys. Chem. B 109 (2005) 6103–6110.
[125] H. Tokuda, K. Ishii, M.A.B.H. Susan, S. Tsuzuki, K. Hayamizu, M. Watanabe, J. Phys. Chem. B 110 (2006) 2833–2839.
[126] T. Umecky, M. Kanakubo, Y. Ikushima, Fluid Phase Equilibr. 228–229 (2005) 329–333.
[127] Y. Saito, K. Hirai, K. Matsumoto, R. Hagiwara, Y. Minamizaki, J. Phys. Chem. B 109 (2005) 2942–2948.
[128] D. Nama, P.G. Anil Kmar, P.S. Pregosin, T.J. Geldbach, P.J. Dyson, Inorg. Chim. Acta 359 (2006) 1907–1911.
[129] A.D. Headley, N.M. Jackson, J. Phys. Org. Chem. 15 (2002) 52–55.
[130] S.T. Lin, M.F. Ding, C.W. Chang, S.S. Lue, Tetrahedron 60 (2004) 9441–9446.
[131] A. Mele, C.D. Tran, S.H. de Paoli Lacerda, Angew. Chem., Int. Ed. 42 (2003) 4364–4366.
[132] A. Mele, B. Vergani, F. Viani, S.V. Meille, A. Farina, P. Bravo, Eur. J. Org. Chem. (1999) 187–196.
[133] C.J. Dymek Jr., J.J.P. Stewart, Inorg. Chem. 28 (1989) 1472–1476.
[134] K.M. Dieter, C.J. Dymek Jr., N.E. Heimer, J.W. Rovang, J.S. Wilkes, J. Am. Chem. Soc. 110 (1988) 2722–2726.
[135] H.C. Chang, J.C. Jiang, W.C. Tsai, G.C. Chen, S.H. Lin, J. Phys. Chem. B 110 (2006) 3302–3307.
[136] S.A. Katsyuba, P.J. Dyson, E.E. Vandyukova, A.V. Chernova, A. Vidiš, Helv. Chim. Acta 87 (2004) 2556–2565.
[137] N.E. Heimer, R.E. Del Sesto, Z. Meng, J.S. Wilkes, W.R. Carper, J. Mol. Liq. 124 (2006) 84–95.
[138] E.R. Talaty, S. Raja, V.J. Storhaug, A. Dölle, W.R. Carper, J. Phys. Chem. B 108 (2004) 13177–13184.
[139] R.W. Berg, M. Deetlefs, K.R. Seddon, I. Shim, J.M. Thompson, J. Phys. Chem. B 109 (2005) 19018–19025.
[140] Y. Umebayashi, T. Fujimori, T. Sukizaki, M. Asada, K. Fujii, R. Kanzaki, S. Ishiguro, J. Phys. Chem. A 109 (2005) 8976–8982.
[141] K. Fujii, T. Fujimori, T. Takamuku, R. Kanzaki, Y. Umebayashi, S. Ishiguro, J. Phys. Chem. B 110 (2006) 8179–8183.
[142] J.N.A. Canongia Lopes, A.A.H. Pádua, J. Phys. Chem. B 110 (2006) 7485–7489.
[143] M. López-Pastor, M.J. Ayora-Cañada, M. Valcárcel, B. Lendl, J. Phys. Chem. B 110 (2006) 10896–10902.
[144] L. Cammarata, S.G. Kazarian, P.A. Salter, T. Welton, Phys. Chem. Chem. Phys. 3 (2001) 5192–5200.
[145] C.D. Tran, S.H. De Paoli Lacerda, D. Oliveira, Appl. Spectrosc. 57 (2003) 152–157.
[146] K. Matsumoto, R. Hagiwara, Y. Ito, S. Kohara, K. Suzuya, Nucl. Instrum. Meth. B. 199 (2003) 29–33.
[147] R. Hagiwara, K. Matsumoto, T. Tsuda, Y. Ito, S. Kohara, K. Suzuya, H. Matsumoto, Y. Miyazaki, J. Non-Cryst. Solids 312–314 (2002) 414–418.
[148] C. Hardacre, J.D. Holbrey, S.E.J. McMath, D.T. Bowron, A.K. Soper, J. Chem. Phys. 118 (2003) 273–278.
[149] C. Hardacre, S.E.J. McMath, M. Nieuwenhuyzen, D.T. Bowron, A.K. Soper, J. Phys.: Condens. Matter 15 (2003) S159–S166.
[150] M. Deetlefs, C. Hardacre, M. Nieuwenhuyzen, A.A.H. Padua, O. Sheppard, A.K. Soper, J. Phys. Chem. B 110 (2006) 12055–12061.
[151] S.M. Urahata, M.C.C. Ribeiro, J. Chem. Phys. 120 (2004) 1855–1863.
[152] C. Rey-Castro, L.F. Vega, J. Phys. Chem. B 110 (2006) 14426–14435.
[153] C.G. Hanke, R.M. Lynden-Bell, J. Phys. Chem. B 107 (2003) 10873–10878.
[154] C.G. Hanke, N.A. Atamas, R.M. Lynden-Bell, Green Chem. 4 (2002) 107–111.
[155] R.M. Lynden-Bell, N.A. Atamas, A. Vasilyuk, C.G. Hanke, Mol. Phys. 100 (2002) 3225–3229.
[156] A. Chaumont, E. Engler, G. Wipff, Inorg. Chem. 42 (2003) 5348–5356.
[157] A. Chaumont, G. Wipff, Phys. Chem. Chem. Phys. 5 (2003) 3481–3488.
[158] Y. Shim, J. Duan, M.Y. Choi, H.J. Kim, J. Chem. Phys. 119 (2003) 6411–6414.
[159] D.D. Zorn, J.A. Boatz, M.S. Gordon, J. Phys. Chem. B 110 (2006) 11110–11119.
[160] S. Takahashi, L.A. Curtiss, D. Gosztola, N. Koura, M.-L. Saboungi, Inorg. Chem. 34 (1995) 2990–2993.
[161] S. Takahashi, K. Suzuya, S. Kohara, N. Koura, L.A. Curtiss, M.-L. Saboungi, Z. Phys. Chem. 209 (1999) 209–221.
[162] C.G. Hanke, A. Johansson, J.B. Harper, R.M. Lynden-Bell, Chem. Phys. Lett. 374 (2003) 85–90.
[163] P.A. Hunt, I.R. Gould, J. Phys. Chem. A 110 (2006) 2269–2282.
[164] M.G. Del Pópolo, R.M. Lynden-Bell, J. Kohanoff, J. Phys. Chem. B 109 (2005) 5895–5902.
[165] M.S. Sitze, E.R. Schreiter, E.V. Patterson, R.G. Freeman, Inorg. Chem. 40 (2001) 2298–2304.
[166] O. Borodin, G.D. Smith, J. Phys. Chem. B 110 (2006) 11481–11490.
[167] M. Bühl, A. Chaumont, R. Schurhammer, G. Wipff, J. Phys. Chem. B 109 (2005) 18591–18599.
[168] T.G.A. Youngs, M.G. Del Pópolo, J. Kohanoff, J. Phys. Chem. B 110 (2006) 5697–5707.
[169] M.G. Del Pópolo, G.A. Voth, J. Phys. Chem. B 108 (2004) 1744–1752.

[170] K.E. Gutowski, J.D. Holbrey, R.D. Rogers, D.A. Dixon, J. Phys. Chem. B 109 (2005) 23196–23208.

[171] C. Cadena, Q. Zhao, R.Q. Snurr, E.J. Maginn J. Phys. Chem. B 110 (2006) 2821–2832.

[172] T. Yan, C.J. Burnham, M.G. Del Pópolo, G.A. Voth, J. Phys. Chem. B 108 (2004) 11877–11881.

[173] J.Z. Yang, Y. Jin, W.G. Xu, Q.G. Zhang, S.L. Zang, Fluid Phase Equilibr. 227 (2005) 41–46.

[174] J.Z. Yang, P. Tian, W.G. Xu, B. Xu, S.Z. Liu, Thermochim. Acta 412 (2004) 1–5.

[175] B.L. Bhargava, S. Balasubramanian, Chem. Phys. Lett. 417 (2006) 486–491.

[176] C.K. Larive, M. Lin, B.S. Kinnear, B.J. Piersma, C.E. Keller, W.R. Carper, J. Phys. Chem. B 102 (1998) 1717–1723.

[177] W.R. Carper, J.L. Pflug, J.S. Wilkes, Inorg. Chim. Acta 202 (1992) 89–93.

[178] N.E. Heimer, J.S. Wilkes, P.G. Wahlbeck, W.R. Carper, J. Phys. Chem. A 110 (2006) 868–874.

[179] I. Nicotera, C. Oliviero, W.A. Henderson, G.B. Appetecchi, S. Passerini, J. Phys. Chem. B 109 (2005) 22814–22819.

[180] M. Castriota, T. Caruso, R.G. Agostino, E. Cazzanelli, W.A. Henderson, S. Passerini, J. Phys. Chem. A 109 (2005) 92–96.

[181] H. Katayanagi, S. Hayashi, H. Hamaguchi, K. Nishikawa, Chem. Phys. Lett. 392 (2004) 460–464.

[182] K. Dahl, G.M. Sando, D.M. Fox, T.E. Sutto, J.C. Owrutskye, J. Chem. Phys. 123 (2005) 084504.

[183] F.R. Trouw, D.L. Price, Annu. Rev. Phys. Chem. 50 (1999) 571–601.

[184] P.J. Dyson, J.S. McIndoe, D. Zhao, Chem. Commun. (2003) 508–509.

[185] S. Dorbritz, W. Ruth, U. Kragl, Adv. Synth. Catal. 347 (2005) 1273–1279.

[186] N. Kuhn, M. Walker, M. Steimann, Z. Naturforsch. 57b (2002) 248–250.